

The effect of Coulomb losses on the relative abundance of heavy and ultraheavy ions in solar energetic particle events

Yulia Kartavykh*, Wolfgang Dröge[†], Berndt Klecker[‡], Leon Kocharov[§],
Gennady Kovaltsov* and Eberhard Möbius[¶]

**Ioffe Physical-Technical Institute, St. Petersburg 194021, Russia*

[†]*Institut für Theoretische Physik und Astrophysik, Universität Würzburg, 97074 Würzburg, Germany*

[‡]*Max-Planck-Institut für extraterrestrische Physik, Garching, Germany*

[§]*Department of Physics, University of Turku, FI-20014 Turku, Finland*

[¶]*Space Science Center and Department of Physics, University of New Hampshire, Durham, NH 03824*

Abstract. The acceleration efficiency for ions with charge Q is a function of their charge to mass ratio Q/A . So far considerations of particle acceleration were restricted by tabulated values of ionization and recombination coefficients which were available only for a limited set of ions, i.e., elements with nuclear charge $Z < 30$. Applying a new method to calculate ionization and recombination rates for ions with arbitrary mass number and charge we consider acceleration including charge transfer for ions with a wide range of their nuclear charge. We demonstrate that due to their considerably smaller Coulomb losses ultra-heavy ions are significantly enhanced with respect to lighter ions. We estimate the magnitude of the possible enrichment of heavier ions due to this effect.

Keywords: acceleration of particles – atomic processes – solar flares

I. INTRODUCTION

Recent observations have revealed very large enhancements of ultraheavy (atomic mass number $A > 70$) elements relative to lighter elements in impulsive Solar Energetic Particle (SEP) events (at energies ≥ 0.15 MeV nucleon⁻¹) [1], [2], [3]. The observed enrichment of heavy nuclei relative to oxygen was ~ 40 for mass 78-100 amu, ~ 120 for mass 125-150 amu, and ~ 215 for 180-220 amu at the energy about 0.3 MeV nucleon⁻¹. The acceleration efficiency for an ion with charge Q is a function of its charge to mass ratio Q/A . It was shown that the inclusion of processes that change the ion charge state (ionization and recombination) into the acceleration models is required at the conditions typical for solar flare plasmas [4], [5], [6], [7]. Recently, such models (so-called charge-consistent acceleration models), which cover the charge states for ions lighter than Ni, were proposed for both, stochastic [8], [9], [10] and shock acceleration [11], [12]. The charge-consistent acceleration models have also been applied to derive the conditions in the acceleration sites for several solar energetic particle events [13], [14], [15]. These calculations were restricted to species with known coefficients for their ionization and recombination cross

sections, which then allowed to infer the corresponding ionization and recombination rates.

With the recent observation of ultraheavy ions in a number of solar energetic particle events the calculation of their energy spectra and charge states has also become important. Their huge overabundance in combination with a potentially quite different Q/A compared to lighter ions pose new constraints on fractionation models for impulsive solar particle events. To compute the charge states and thus Q/A for these species the corresponding cross sections or a reliable method to infer them is needed. Recently, a simplified method for the calculation of ionization and recombination rates for ions with a given nuclear charge Z and the ion charge Q was described [16]. In the present work we use the calculated ionization and recombination rates for tellurium (Te, $Z = 52$, $A = 128$) and compute additionally the same rates for krypton (Kr, $Z = 36$, $A = 84$). For these ions we demonstrate that the observed overabundance of ultraheavy ions can be explained by reduced Coulomb losses in comparison with lighter ions.

II. CALCULATION OF IONIZATION AND RECOMBINATION RATES

Charge states of accelerated ions are formed as a result of competing ionization and recombination processes. There are two main contributions to the ionization: collisions with thermal electrons and collisions with thermal protons (and α -particles) of the ambient plasma. Recombination consists of two terms: radiative and dielectronic recombination. The ionization and recombination rates can be obtained by a convolution of the corresponding cross section, and the velocity distribution function of ambient particles [17], [18].

Usually some approximations of the corresponding cross sections are used to calculate the ionization rates due to collisions with electrons, e.g., [19]. In these papers the partial cross sections for individual electron shells were presented as a function of the ratio of the incident electron's energy and the ionization potential of a certain electron shell, with the coefficients, which were specified for each charge state of the ion. Such coefficients are

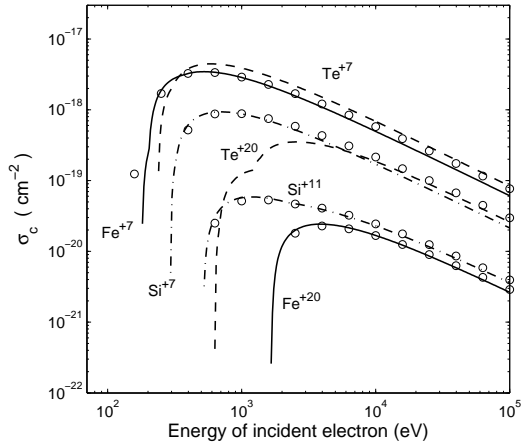


Fig. 1: Electron' ionization cross sections of Si^{+7} , and Si^{+11} (dashed-dotted line) Fe^{+7} , Fe^{+20} (solid line) and Te^{+7} , Te^{+20} (dashed line), calculated by the present approach. Ionization cross sections of Si^{+7} , Si^{+11} and Fe^{+7} , Fe^{+20} calculated in accordance with [19] are shown as open circles.

known only for a limited number of elements (from H to Ni). In our recent work [16] we follow the more general approximations of [20], [21], [22]. Cross sections are deduced as generic functions of the energy of incident electrons, of ionization potentials of a given subshell, and of a certain electron structure which is defined by the principal and orbital quantum numbers. The accuracy of the approach taken above was checked by comparison of the calculated ionization cross sections with the ones obtained for Si and Fe making use of the approach given by [23] and [19]. Figure 1 shows that the two approaches result in consistent cross sections for Fe and Si. The cross sections for Te^{+7} and Te^{+20} are also given on the figure for comparison. The calculated ionization potentials allowed us also to calculate the cross sections of recombination and proton-impact ionization. The details, how the cross section and charge changing rates were obtained are given in [16].

The equilibrium mean charge Q_{eq} which is a function of the ion energy E and the temperature of the surrounding plasma T is reached when an ion has moved through a plasma for a sufficiently long time [17], [18]. It is defined by a balance between ionization and recombination processes and depends on the ion energy E and on the temperature of the surrounding plasma T . This is illustrated in Figure 2 which shows the ionization and recombination rates for Te^{+20} and Te^{+21} , respectively, along with the equilibrium charge state as a function of energy. It can be seen that, when these rates become equal to each other at an energy of ≈ 0.4 MeV nucleon $^{-1}$, the equilibrium charge state of Te reaches the value of 20. The equilibrium mean charge is important for understanding the charge state of accelerated ions, because their mean charge is between its thermal and equilibrium values. The equilibrium charges of Kr and Te, calculated in accordance with methodics [16] together with Q_{eq} for Fe are shown in Figure 3.

III. ACCELERATION MODEL

For the treatment of particle stochastic acceleration, stripping and escape from the acceleration region we numerically solve the equation [24]:

$$\begin{aligned} \frac{\partial f_i}{\partial t} = & \frac{1}{p^2} \frac{\partial}{\partial p} \left(p^2 D_p \frac{\partial f_i}{\partial p} \right) - \frac{1}{p^2} \frac{\partial}{\partial p} \left(p^2 \left(\frac{dp}{dt} \right)_c f_i \right) \\ & + \frac{\partial}{\partial x} \left(K_x \frac{\partial f_i}{\partial x} \right) - n(S_i + \alpha_i) f_i \\ & + nS_{i-1} f_{i-1} + n\alpha_{i+1} f_{i+1} \end{aligned} \quad (1)$$

where $f_i(p, x, t)$ is the distribution function for ions of the i -th ionization state, S_i and α_{i+1} are ionization and recombination rate coefficients, n is the density of the ambient electrons, and p is the momentum per nucleon. The diffusion coefficients in momentum (D_p) and coordinate (K_x) space due to scattering of particles with charge Q and atomic mass number A by Alfvén wave turbulence can be cast into the form [25], [26]: $D_p = D_0 (Q/A)^{2-S} p^{S-1}$, $K_x = K_0 (Q/A)^{S-2} p^{3-S}$, if $S < 2$, and $K_x = K_0 (Q/A)^{S-2} p$, if $S \geq 2$. Here S is the power law index for spectral energy density of the turbulence. The term $(dp/dt)_c$ describes the energy losses due to Coulomb collisions. The solution of this equation is governed by the ratios of the characteristic time scales τ_A/τ_D , the product $\tau_A n$, the plasma temperature T used to specify the initial charge distribution and the ionization/recombination rates, and the spectral index of turbulence, S . Here $\tau_A = p^2/D_p \propto (Q/A)^{S-2}$ and $\tau_D = L^2/K_x \propto (Q/A)^{2-S}$ are the characteristic acceleration and diffusion times. Note that the values τ_A/τ_D and $\tau_A n$ given below are related to the energy 1 MeV nucleon $^{-1}$. Here L is the size of the acceleration region. The ratio τ_A/τ_D characterises the acceleration and defines the shape of the energy spectra of accelerated ions without Coulomb losses - the smaller its value the harder the spectrum. The product $\tau_A n$ determines the significance of the Coulomb losses, the rates of charge

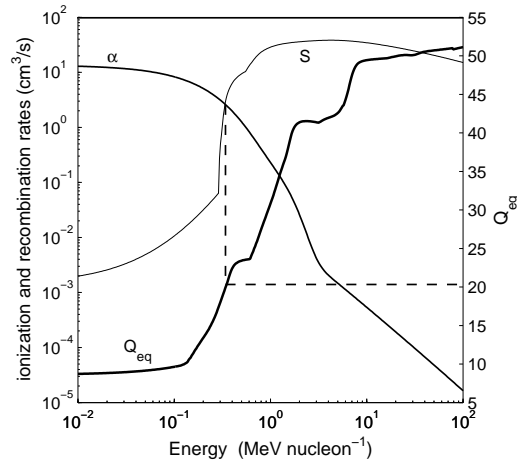


Fig. 2: Ionization rate (S) for Te^{+20} and recombination rate (α) for Te^{+21} together with the equilibrium mean charge (Q_{eq}) at $T=10^6$ K. The vertical dashed line indicates the energy where $\alpha = S$ and connects to the corresponding value of Q_{eq}

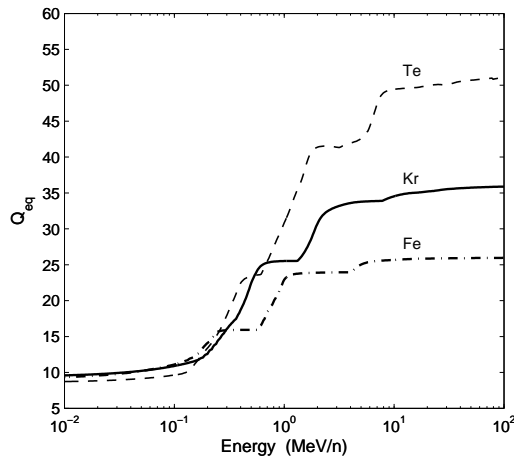


Fig. 3: Equilibrium mean charge of Fe, Kr and Te, $T = 10^6$ K.

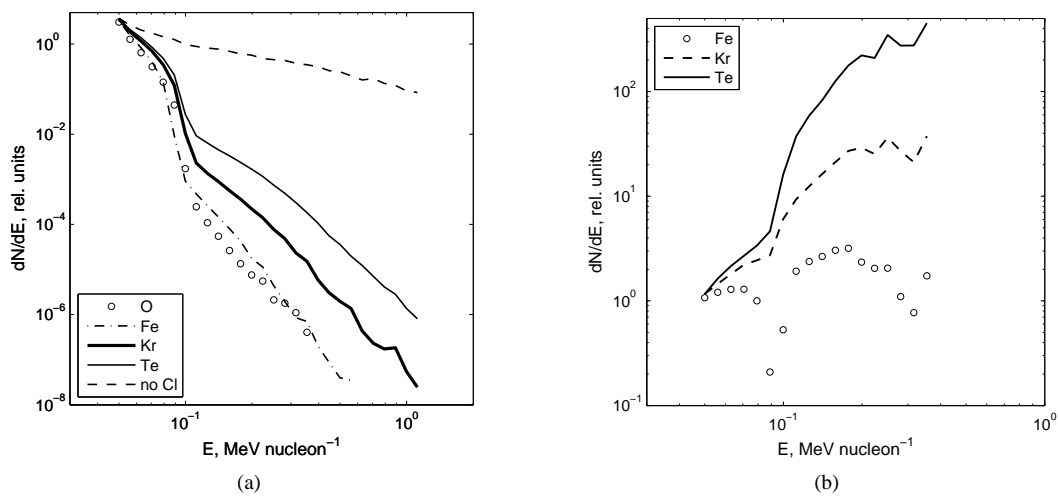


Fig. 4: (a) Energy spectra of O, Fe, Kr and Te. Parametrs are given in the text. (b) Ratios Fe/O, Kr/O, Te/O, if Coulomb losses are included.

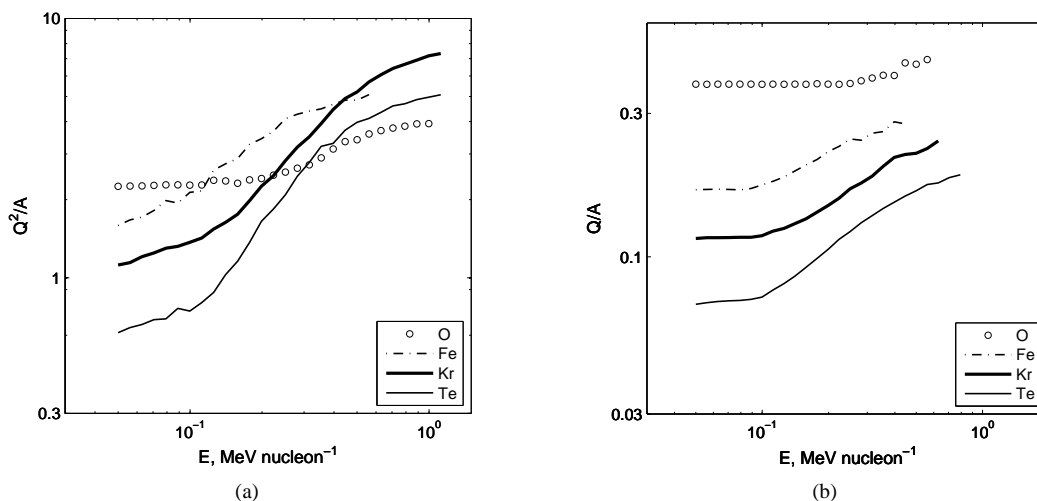


Fig. 5: (a) Q^2/A of O, Fe, Kr and Te ions, if Coulomb losses are absent. (b) Q/A of O, Fe, Kr and Te ions, Coulomb losses are included.

changing processes and, therefore, $\langle Q^{acc}(E) \rangle$ as well.

IV. RESULTS AND DISCUSSION

We study the case $S = 2$, when $\tau_A/\tau_D = \text{const}(Q/A)$ and without Coulomb losses energy spectra of all ions are the same (Figure 4a). It shows energy spectra of O, Fe, Kr and Te ions (summed over all charge states) under the parameters: $\tau_A/\tau_D = 1.0$, $\tau_A n = 5 \times 10^{11} \text{ s cm}^{-3}$, $S = 2$, $T = 10^6 \text{ K}$, if Coulomb losses are taken into account, and if they are absent (dashed curve). It is seen that Coulomb losses are most important for lighter ions (like O). The enhancement factors for Fe, Kr and Te due to only Coulomb losses are shown in Figure 4b. Under the selected parameters in the energy range $0.2 - 0.5 \text{ MeV/nucleon}$ the enhancements relative to O were ~ 2 for Fe, ~ 30 for Kr (representative for the mass range 78-100 amu), ~ 250 for Te (mass group 125-150 amu). Note, that a decrease of the parameter $\tau_A n$ by a factor of 5 (i.e. $\tau_A n = 10^{11} \text{ s cm}^{-3}$) results in enhancement factor of 1.1. Figure 5 shows the ratio Q^2/A , which would be the appropriate parameter to study selective acceleration, if Coulomb losses are not included (5a), and Q/A , which is the controlling parameter if Coulomb losses are taken into account (5b). It is seen, that the ratio Q/A is always lower for heavy elements, which enables their additional preferential acceleration.

Our model calculations show the importance of charge stripping and Coulomb losses for heavy ion energy spectra at $E > 0.1 \text{ MeV/nucleon}$. Our results suggest that the overabundance of heavy ions in the mass range ~ 80 to 150 can be accounted for by Q^2/A dependent Coulomb losses. In the mass range 30 - 60, however, other processes as resonant or non-resonant wave particle interactions (e.g. [27], and references therein) may play an important role.

ACKNOWLEDGMENT

Y.K. and G.K. thank Russian Foundation for basic research for partial support (project No. 09-02-00019-a)

REFERENCES

- [1] Reames, D.V. 2000, *ApJ*, 540, L111
- [2] Mason, G.M., Mazur, J.E., Dwyer, J.R., Jokipii, J.R., Gold, R.E., Krimigs, S.M. 2004, *ApJ*, 606, 555
- [3] Mason, G.M. *SpaceSc.Rev.*, 2007, 130, 231
- [4] Ostryakov, V.M., & Stovpyuk, M.F. 1997, *AstronomyReports*, 41, 386
- [5] Ruffolo, D. 1997, *ApJ*, 481, L119
- [6] Barghouty, A.F., & Mewaldt, R.A. 1999, *ApJ*, 520, L127
- [7] Kocharov, L., Kovaltsov, G.A., Torsti, J. 2001, *ApJ*, 556, 919
- [8] Kartavykh, Yu.Yu., Ostryakov, V.M., Stepanov, I.Yu., Yoshimori, M. 1998, *CosmicResearch*, 36, 437
- [9] Ostryakov, V.M., Kartavykh, Y.Y., Ruffolo, D., Kovaltsov, G.A., Kocharov, L. 2000, *J.Geophys.Res.* 105(A12), 27315
- [10] Kartavykh, Yu.Yu., Wannawichian, S., Ruffolo, D. Ostryakov, V.M. 2002, *Adv.SpaceRes.* 30(1), 119
- [11] Stovpyuk, M.F., & Ostryakov, V.M. 2001, *SolarPhysics*, 198, 163
- [12] Lytova, M.F., Kocharov, L. 2005, *ApJ*, 620, L55
- [13] Kartavykh, J.J., Dröge, W., Kovaltsov, G.A., & Ostryakov, V.M. 2005, *SolarPhys.*, 227, 123
- [14] Dröge, W., Kartavykh, Y.Y., Klecker, B., & Mason, G.M. 2006, *ApJ*, 645, 1516
- [15] Kartavykh, Y.Y., Dröge, W., Klecker, B., Mason, G.M., Möbius, E., Popecki, M., & Krucker, S. 2007, *ApJ*, 671, 947
- [16] Kartavykh, Y.Y., Dröge, W., Klecker, B., Kocharov, L., Kovaltsov, G.A., Möbius, E. 2008, *ApJ*, 681, 1653
- [17] Luhn, A., & Hovestadt, D. 1987, *ApJ*, 317, 852
- [18] Kocharov, L., Kovaltsov, G.A., Torsti, J., Ostryakov, V.M. 2000, *A&A*, 357, 716
- [19] Arnaud, M., & Raymond, J. 1992, *ApJ*, 398, 394
- [20] Sampson, D.H., & Golden, L.B. 1978, *J.Phys.B:At.Mol.Phys.*, 11, 541
- [21] Golden, L.B., & Sampson, D.H. 1980, *J.Phys.B:At.Mol.Phys.*, 13, 2645
- [22] Clark, R.E.H., & Sampson, D.H. 1984, *J.Phys.B:At.Mol.Phys.*, 17, 3311
- [23] Arnaud, M., & Rothenflug, R. 1985, *A&AS*, 60, 425
- [24] Kartavykh, J.J., Dröge, W., Kovaltsov, G.A., & Ostryakov, V.M. 2006, *Adv.Sp.Res.*, 38, 516
- [25] Hasselmann, K., & Wibberenz, G. 1968, *Z.Geophys.*, 34, 353
- [26] Schlickeiser, R., & Steinacker, J. 1989, *SolarPhys.*, 122, 29
- [27] Miller, J.A. 1998, *SpaceScienceRev.*, 86, 79